Title
Optimization of surface passivation for suppressing leakage current in GaSb PIN devices

Author
Ji, Yihong

Publication Date
2020

UNIVERSITY OF CALIFORNIA

Los Angeles

Optimization of surface passivation for suppressing leakage current in GaSb PIN devices

A thesis submitted in partial satisfaction

of the requirements for the degree Master of Science

in Materials Science and Engineering

by

Yihong Ji

2020

ABSTRACT OF THE THESIS

Optimization of surface passivation for suppressing leakage current

in GaSb PIN devices

by

Yihong Ji

Master of Science in Materials Science and Engineering

University of California, Los Angeles, 2020

Professor Dwight C. Streit, Chair

The suppression of leakage current via surface passivation plays a critical role for GaSb based optoelectronic devices. In this study, the sulfur passivation parameters are carefully optimized in this study for improving the performance of GaSb p-i-n devices. Two competing processes are evaluated during the sulfur passivation process: the hydrolysis and oxidation of HS^- ions that aide surface passivation and re-oxidation, respectively. Upon the optimization of sulfur passivation parameters and subsequent encapsulation with ALD Al_2O_3, the surface resistivity significantly increased from $4.3k\Omega \cdot cm$ to $28.6k\Omega \cdot cm$, leading to 19.1 times drop in dark current at room temperature for the GaSb p-i-n structure. This work provides a repeatable and stable passivation approach for improving the optoelectronic performance of GaSb based devices.

This thesis of Yihong Ji is approved.

Jaime Marian

Arion-Xenofon Hadjioannou

Dwight C. Streit, Committee Chair

University of California, Los Angeles

2020

This thesis is dedicated to my family, to the people who trusted me and helped me once in my life.

Table of Contents

List of Figures

Acknowledgments

I would first like to thank my research advisor Dr. Baolai Liang and Prof. Arion-Xenofon Hadjioannou, for their tremendous help and guidance over the course of my research and Master study at UCLA. I am really grateful to them for offering me such a precious research opportunity to work on the photodetector project, for giving me great support throughout my research. I also appreciate the guidance and instructions from the remainder of my committee, Prof. Dwight C. Streit and Prof. Jaime Marian.

I would like to thank to my group members, Dr. Khalifa M. Azizur-Rahman and Tingyuan Chang, for teaching me the invaluable knowledge of device fabrication and characterization. I appreciate the advice offered by them during past discussion.

I would like to acknowledge the financial support from the National Science Foundation (ECCS-1810507).

In the end, I would like to thank my parents and my family, for their endless love, support and care in my life.

1. Introduction

The GaSb nanostructures are widely applied in thermo-photovoltaic cells, solar cells and photodetectors due to their high carrier mobility and bandgap engineering flexibility.[1-6] However, the unpassivated GaSb devices are prone to high trap state density from unterminated dangling bonds and native oxides. These native oxides are formed via the following reactions:[7]

$$2\,GaSb + 3O_2 \rightarrow Ga_2O_3 + Sb_2O_3 \quad (1)$$

$$2\,GaSb + Sb_2O_3 \rightarrow Ga_2O_3 + 4\,Sb \quad (2)$$

These dangling bonds and oxide layers give rise to high surface state density and Fermi level pinning within the bandgap[8] that increases the surface recombination velocity (leading to large surface leakage current) and deteriorates the opto-electronic performance of as-fabricated devices. The suppression of surface leakage current is thus highly desirable for GaSb-based optoelectronics.

Chemical sulfur passivation has proven to be an effective way to reduce surface leakage current and is widely used in GaAs based devices.[9-13] Generally, the sulfur passivation can be achieved by immersing the device into ammonium sulfide $(NH_4)_2S$ solution, where the dangling bonds on the device surface can be saturated by the sulfur species, i.e. HS^- and H_2S, after the removal of the native oxide layer through the following reactions:

$$A^{III}B^{V} + HS^- + H_2O \rightarrow (A^{III})_{x'}S_{y'} + (B^{V})_{x''}S_{y''} + OH^- + H_2\uparrow \ [14] \quad (3)$$

$$A^{III}B^{V} + H_2S \rightarrow (A^{III})_{x'}S_{y'} + (B^{V})_{x''}S_{y''} + H_2\uparrow \ [11] \quad (4)$$

A thin sulfide monolayer will then be formed on the device surface that terminates the surface dangling bonds, which increases shunt resistance and decreases carrier recombination on the

surface. Though improvements of electrical and optical performance due to this mechanism have been observed, [15-18] it should be noted that this aqueous-based chemical reaction is influenced by different parameters such as dilution ratio, pH, temperature, and passivation time.

In this study, the impacts of these parameters on the GaSb p-i-n devices were investigated upon ammonium sulfide $(NH4)_2S$ passivation. The suppression of leakage current was at first deduced by comparing pre- and post-treatment current density-voltage (J-V) characteristics on p-i-n GaSb on GaAs substrate (will be referred to as GaSb/GaAs) devices. We observed that the surface resistivity increased by 3-orders and dark current dropped 16.1 folds at room temperature through the optimization of sulfur passivation parameters. To determine the efficacy of the passivation scheme, it was further applied to p-i-n GaSb on GaSb substrate (will be referred to as GaSb/GaSb) device. A similar reduction of dark current was also observed. Finally, the influence of Al_2O_3 on the reduction and stability of surface passivation was also studied. A stable passivated surface without degradation was obtained upon Al_2O_3 deposition. Based on a combination of modified sulfur passivation and Al_2O_3 deposition, the surface resistivity increased by more than 6.7 folds and leakage current dropped by 19.1 folds for p-i-n GaSb/GaSb device at room temperature.

2. Experimental section

2.1 Device design and growth via Molecular-beam epitaxy (MBE)

The GaSb p-i-n devices shown in Figure 2-1 were grown on the semi-insulating (SI) GaAs (100) and GaSb (100) via a Veeco Gen930 solid-source molecular-beam epitaxy (MBE) reactor, respectively.

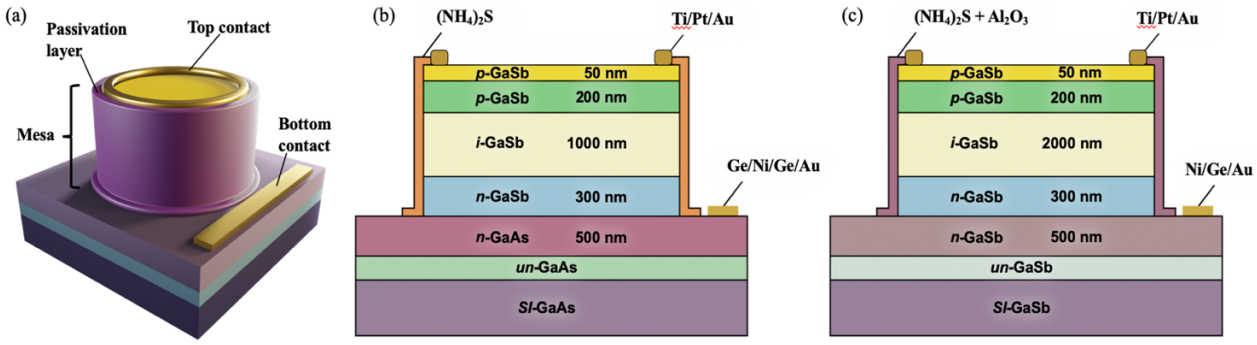

Figure 2-1 Schematic diagram of (a) mesa structure with passivation. Detailed layer structure of GaSb p-i-n devices grown on (b) GaAs (100) and (c) GaSb (100) are also presented.

For the heterostructure in Figure 2-1(a), the GaSb p-i-n devices layers were grown at 500 ℃ with the Sb/Ga beam equivalent pressure (BEP) ratio of 6 via interfacial-misfit (IMF) growth technology.[19] The GaSb p-i-n structure in Figure 2-1(b) was also grown at 500 ℃ under similar conditions, but on GaSb (100) substrate after the removal of native oxide layer at 540 ℃. Tellurium (Te) and Beryllium (Be) were used as the p-dopants and n-dopants for both GaSb p-i-n devices, respectively. Because as-grown GaSb layers were measured to have an acceptor concentration of ~$7 \times 10^{16}\ cm^{-3}$, n-doping compensation were implemented for both devices through using Te in

order to reduce the electronic noise. The minimum background doping level of $6 \times 10^{16}\ cm^{-3}$ and $2 \times 10^{16}\ cm^{-3}$ were achieved after the compensation.

2.1 Device fabrication and characterization

Mesa devices with different diameters, 100, 200 and 400μm, were fabricated through standard photolithographic process. Ge/Ni/Ge/Au and Ni/Ge/Au layers were used for n-GaAs and n-GaSb contacts, respectively. In order to obtain a good electrical contact, HCl (37%): H_2O= 1: 1 etching solution was used to remove the native oxide layer before metal deposition. The samples used in this study, prior to different passivation treatments, were all from the same growth batch and fabricated together for fair comparison. Since, oxygen forms more stable and stronger Ga-O and Sb-O bonds compared to Ga-S and Sb-S, HCl polishing is required before sulfur passivation. The surface native oxide layers were removed by immersion in HCl (37%): H_2O: IPA mixed solution with the ratio of 3: 2: 1 for 30 seconds, followed by 5 seconds of de-ionized water (DI) dip and N_2 blow dry. The polished samples were then quickly transferred into ammonium sulfide $(NH_4)_2S$ solution. After passivation, the samples were dipped for 10 seconds in DI water and N_2 blow dry. All dark current measurements after sulfur passivation were conducted by using High-frequency Probe Station and Agilent 4156C semiconductor parameter analyzer at room temperature. A 30 nm Al_2O_3 layer was deposited on sulfur passivated GaSb/GaSb device after I-V measurement by using Atomic Layer Deposition (ALD) at 200℃ substrate temperature.

3. Results Discussions

3.1 Surface passivation for GaSb/GaAs heterostructure device

3.1.1 The influence of $(NH_4)_2S$ solution conditions on the effect of passivation

Figure 3-1 shows the dark current density with respect to voltage curves after different sulfur passivation treatments. Only one variable was changed for each passivation scheme to ensure the validity of the comparison. The first passivation was conducted in a saturated $(NH_4)_2S$ solution at room temperature for 15 minutes, as can be seen from Figure 3-1(a). The elimination of native oxide after HCl polishing reduced the surface states, leading to a drop in dark current. However, the dark current unexpectedly increased after initial sulfur passivation. This can be explained through examining the solution chemistry. In $(NH_4)_2S$ solution, both NH_4^+ and S^{2-} ions will hydrolyse into $(NH_3)\cdot H_2O$ and HS^- through the following reactions:

$$NH_4^+ + H_2O \rightleftharpoons (NH3)\cdot H_2O + H^+ \quad (5)$$

$$S^{2-} + H_2O \rightleftharpoons HS^- + OH^- \quad (6)$$

The HS^- ions can further hydrolyze and form H_2S gas:

$$HS^- + H_2O \rightleftharpoons H_2S_{(g)} + OH^- \quad (7)$$

This reaction however is limited under room temperature or in concentrated solution.[20] Additionally, the HS^- is unstable when oxygen is present and will partly oxidize into thiosulfate ($S_2O_3^{2-}$): [21]

$$2HS^- + 2O_2 \rightarrow S_2O_3^{2-} + H_2O \quad (8)$$

The +6-valency of the central S ion in $S_2O_3^{2}$ makes it a highly oxidizing agent.[22] Therefore, when treating the sample with high concentration $(NH_4)_2S$ solution, as in this case, the polished sample surface was re-oxidized by $S_2O_3^{2}$ and lead to an increase of leakage current. The oxidation of the surface in concentrated sulfur solution was also observed from XPS measurement study on SiGe, where it was proposed that sulfite and thiosulfate adsorb onto the surface and promote surface oxidation.[23]

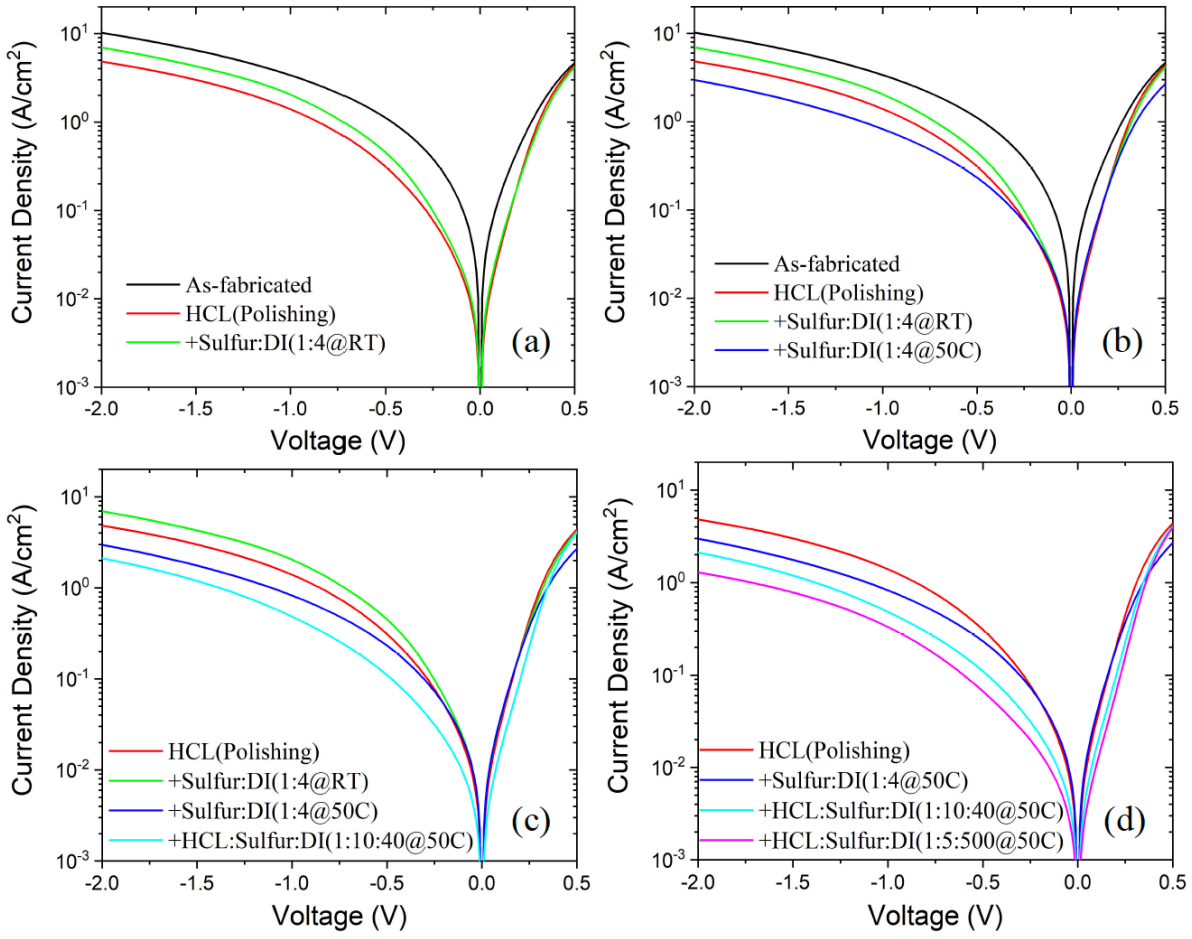

Figure 3-1 Comparisons of J-V curves (@298K) for 400μm GaSb/GaAs p-i-n devices treated by (a) $(NH_4)_2S$: H_2O with the ratio of 1: 4 at 25℃ for 15 minutes, (b) $(NH_4)_2S$: H_2O with the ratio of 1: 4 at 50℃ for 15 minutes, (c) HCl: $(NH_4)_2S$: H_2O with the ratio of 0.1: 1: 4 at 50℃ for 15 minutes, (d) HCl: $(NH_4)_2S$: H_2O with the ratio of 1: 5: 500 at 50℃ for 15 minutes.

Besides HS^- ions, H_2S gas is another sulfide that contributes to the surface passivation. Since aqueous HS^- is not as effective as we expected, we surmised that the increase of H_2S gas may enhance the effect of sulfur passivation. The restricted reaction (7) can be realized at elevated temperatures. As can be seen from Figure 3-1(b), the sample shows a drop in dark current, compared with prior treatment (a), after dipping the sample in 50 ℃ $(NH_4)_2S$ solution. Furthermore, a more reactive surface and sulfur species, under the aid of high temperature, may contribute to the drop as well.[24] This observation validated our assumption that H_2S is more effective than HS^- ion in terms of GaSb surface passivation.

Further study was conducted through adding acid into the previous $(NH_4)_2S$: H_2O (1:4) solution. A decrease of dark current can be clearly seen from Figure 3-1(c). We initially assumed that by adding acid to the solution (i) the formation of H_2S gas would be promoted and (ii) acidic environment would prevent the surface from re-oxidizing with $S_2O_3^2$. However, we noticed that the addition of HCl into as-prepared $(NH_4)_2S$ solution made the solution turbid. This can be attributed to the formation of elemental sulfur biproduct when thiosulfate reacts with protons:

$$S_2O_3^{2-} + 2H^+ \rightarrow SO_2 + S_{(s)} + H_2O \quad (9)$$

Since the solution pH remained at 11 after adding 1 mL HCl, the basic environment indicates that the protons are first exhausted thoroughly by thiosulfate before it can react with OH^- or HS. The partial depletion of thiosulfate in the solution leads to a weakening of re-oxidation of the surface further promoting Ga-S and Sb-S bonds, leading to a decrease in leakage current.

Figure 3-1(d) shows the dark J-V characteristics after diluting the $(NH_4)_2S$ solution, a further suppression of leakage current was achieved. Diluting the sulfur solution further promotes reaction (7) leading to an increase of H_2S gas and demotes reaction (8) leading to a decrease in $S_2O_3^{2}$. The pH of HCl: $(NH_4)_2S$: H_2O= 1: 5: 500 solution dropped to 7 from 11. However, making the solution more acidic, from our observation, can damage the metal contact surface. In particular, the solution dielectric constant decreased in the course of dilution, lower dielectric constant favours the formation of covalent bonds between soft acid Lewis centers[25] and the sulfide species, leading to a decrease of surface recombination velocity[26] and thereafter surface leakage current.

3.1.2 The influence of immersion time on the effect of passivation

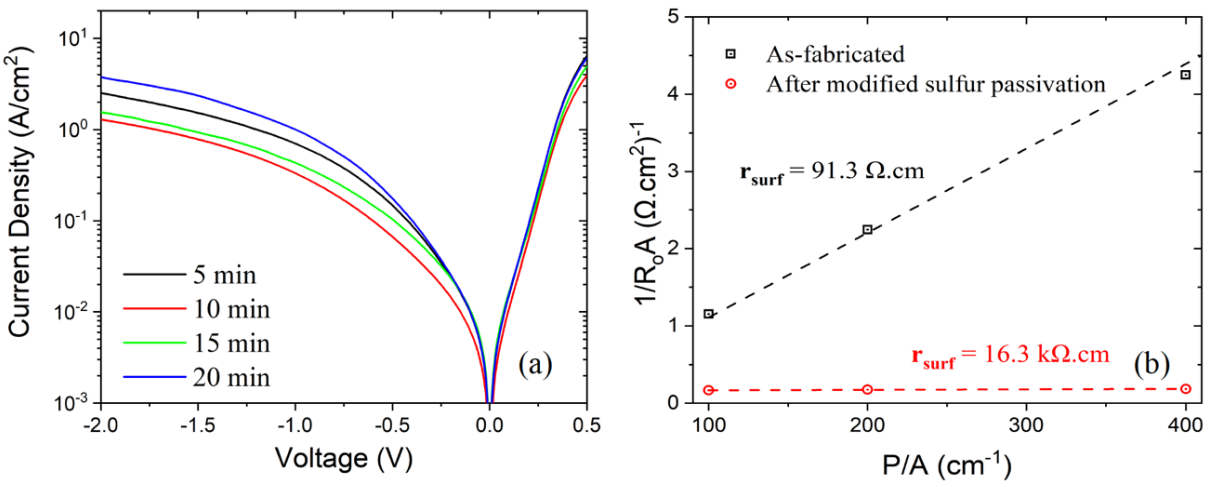

Figure 3-2(a) The influence of different passivation time on the dark current density for d=400μm GaSb/GaAs p-i-n devices (@298K), (b) Comparison of surface resistivity change before and after optimized passivation (HCl: $(NH_4)_2S$: H_2O= 1: 5: 500 @ 50℃ for 10 mins).

Based on the passivation recipe obtained from Figure 3-1(d): HCl: $(NH_4)_2S$: H_2O= 1: 5: 500 at 50℃, we further studied the influence of different immersion time on the surface passivation, as

shown in Figure 3-2(a). If the immersion time is insufficient, e.g. 5 minutes, the surface passivation is not enough, and many dangling bonds remain unterminated. If the immersion is excessive, the oxygen will eventually replace the sulfur on the surface with the existence of $S_2O_3^{2-}$, resulting in the increase of leakage current as indicated by the blue curve in Figure 3-2(a). More importantly, it should be noted that the dark current after 20 minutes passivation is even greater than that of 5 minutes passivation, which means that the GaSb surface is prone to oxidation, monolayer sulfur terminated bonds are replaced by oxygen. The surface resistivity, as shown in Figure 3-2(b), was obtained by fitting the curve of the inversed zero-bias dynamic resistance-area product $1/\ (R_0A)$ as a function of perimeter-to-area ratio P/A:

$$\frac{1}{R_0A} = \left(\frac{1}{R_0A}\right)_{Bulk} + \left(\frac{1}{r_{surface}}\right) \times \frac{P}{A} \tag{10}$$

where the $r_{surface}$ represents the surface resistivity. The surface resistivity increased from $91.3\ \Omega \cdot cm$ to $16.3\ k\Omega \cdot cm$ after the optimized sulfur passivation, indicating a successful suppression of leakage current. The leakage current dropped 16.1 folds at 0.5V reverse bias and the rectification ratio at $\pm$0.5V increased from 0.62 to 1.87.

3.2 Optimized surface passivation for GaSb/GaSb homostructure device

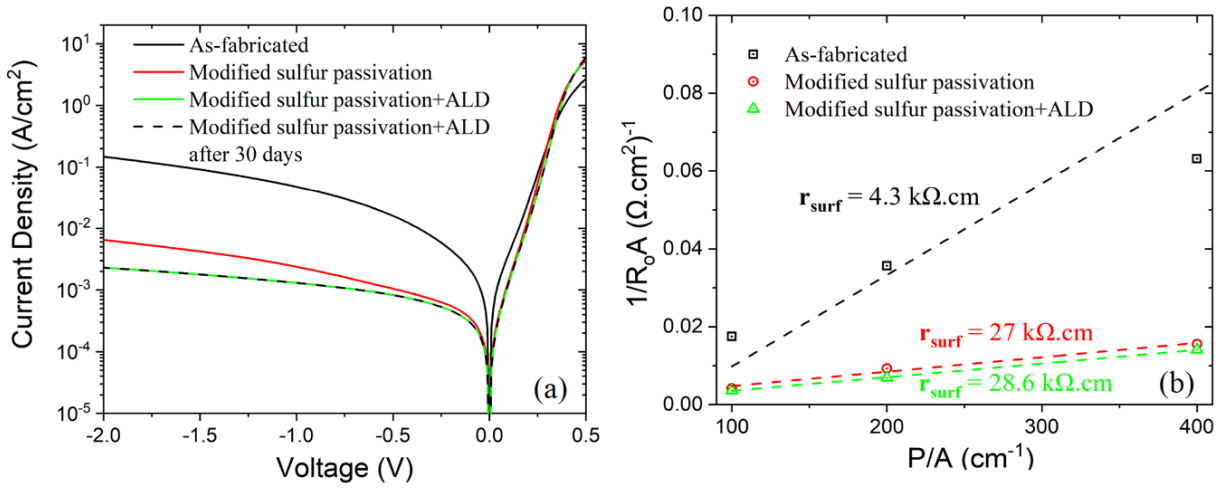

Figure 3-3(a) Dark J-V curves of before and after passivation for d=400μm GaSb/GaSb p-i-n device (@298K), (b) Comparison of surface resistivity change before and after passivation.

To verify the effectiveness and repeatability of this modified surface passivation recipe, we further passivated GaSb/GaSb p-i-n device with 2 μm intrinsic region shown in Figure 2-1(c). The surface leakage current is more dominant in this structure owing to the larger surface-to-volume ratio. Additionally, in GaSb/GaSb homostructures the surface leakage current accounts for a larger fraction of the dark current compared to GaSb/GaAs heterostructures due to the absence of interfacial IMF layers. Interfacial misfit dislocations introduce trap states that increase (Shockley-Read-Hall) SRH generation-recombination current. Figure 3-3(a) shows the dark current density change via the optimized passivation recipe obtained from Figure 3-2(a). A similar reduction (15.1 times drop at 0.5 reverse bias) of dark current was achieved demonstrating the effectiveness of this optimized passivation method. The effects are a by-product of the chemical processes described in Section 3.1, namely oxidation and hydrolysis of HS^- ion leading to a competition between surface passivation and re-oxidation. These two competing reactions are ubiquitous throughout in

the course of passivation, an optimum surface passivation can be realized when the hydrolysis of HS^- ion is favoured and the re-oxidation is inhibited.

Regardless of the improvement in dark current after sulfur passivation, the monolayer film is unstable and desorbs from the sidewall surface over time so that the leakage current reverts to pre-passivation levels. To avert this, a 30 nm Al_2O_3 layer was deposited on the sulfur passivated GaSb/GaSb device sidewall to investigate the influence of Al_2O_3 encapsulation on the desorption of sulfur atoms and surface passivation. As can be seen in Figure 3-3(a), the dark current density was further suppressed after Al_2O_3 deposition, notably at larger reverse bias. This further drop may be attributed to the removal of re-grown oxides after sulfur passivation. Trimethlyaluminum (TMA) precursor,[27] for ALD Al_2O_3 growth, was shown to reduce or "clean-up" In and As native oxides. Similar phenomena can be hypothesized for GaSb passivation as well, where the Al-O interfacially bonds through either supplementing or substituting Sulfur terminated bonds further decreasing surface leakage current. [28-30] More importantly, after measuring the device 30 days later, the leakage current remains the same as that after passivation, suggesting that the encapsulating layer can effectively inhibit the desorption of sulfur atoms. Figure 3-3(b) shows significant increase in surface resistivity after passivation. Compared to the significant increase in surface resistivity after sulfur passivation, the surface resistivity only increases by a small fraction after Al_2O_3 deposition, suggesting that the surface had been very close to be fully passivated through the previous sulfur passivation. The leakage current dropped 19.1 times at 0.5 V reverse bias by combining modified

sulfur passivation and Al_2O_3 encapsulation, leading to the increase of rectification ratio ($\pm$0.5V) from 2.2 to 3.85.

4. Conclusions

The impact of passivation on the GaSb p-i-n device leakage current was investigated upon ammonium sulphide $(NH4)_2S$ passivation. Two competing reactions are inferred to exist throughout the course of passivation: hydrolysis and oxidation of HS^- ions leading to surface passivation and oxidation respectively. Due to the complex reactions on the GaSb surface with $(NH_4)_2S$ solution, a neutral environment, higher temperature, and appropriate immersion time need to be carefully optimized in order to maximize the passivation quality. After the passivation parameters (including temperature, acid, pH, and time) were finalized, the surface resistivity increased significantly, followed by two orders of magnitude decrease in dark current at room temperature for GaSb/GaSb p-i-n photodiodes. Further suppression of leakage current was achieved based on the combination of modified sulfur passivation and Al_2O_3 deposition. This research paves the way for improving the optoelectronic performance of GaSb devices via effective surface passivation process.

5. Appendix. Device Fabrication

5.1 Photolithography

1. Sample piece cleaning: Acetone rinse-> Methanol rinse -> IPA rinse -> N2 dry
2. Hard bake at 150 ℃ for 3 minutes.
3. Spin coating AZ-5214 photoresist on the sample piece.
4. Soft bake at 100 ℃ for 1 minutes.
5. Pattern the sample with different mask by using the Karl Suss Contact Aligner.
6. Develop the exposed area by using AZ-400K developer
7. Descum the photoresist residue by using Matrix Asher at 50 ℃ for 1 minutes.

5.2 Mesa etch

1. Etch the device sample using Unaxis SLR 770 etcher (BCl_3/Ar, 50:10 sccm, RF power = 800W) to the desired device layer. Measure the etch depth using Dektak profiler.
2. Cleaning the etched sample with Acetone and IPA, followed by N_2 blow dry.

5.3 Metal deposition

1. Repeat **5.1**
2. Dip the sample in HCl:H20 = 1:1 for 30 seconds to remove the native oxide before deposition.
3. Quickly load the sample into New CHA e-beam evaporator, deposit appropriate metal as required: Ni/Ge/Au (100:500:1500 Å) for n-GaSb bottom contact, Ge/Ni/Ge/Au (500:100:500:1500 Å) for n-GaAs bottom contact. Ti/Pt/Au (500:500:1000 Å) for Top contact.

4. Lift off the metal layer by immersing sample piece into Acetone for 10 minutes, followed by IPA rinse and N_2 Blow dry.
5. Descum the photoresist residue by using Matrix Asher at 50 ℃ for 1 minutes

5.4 Sidewall passivation

1. Prepare HCl: H2O: IPA = 3: 2: 1 mixed solution and $(NH4)_2S$ solution.
2. Dip sample piece in the mixed solution for 30 seconds to remove native oxide layer on the sidewall surface, followed by 5 seconds DI water rinse.
3. Immerse sample piece into as-prepared $(NH4)_2S$ solution with different treatments (specific procedures are in the Experimental section).
4. After passivation, take the sample out and rinse with DI water, N_2 blow dry.

6. References

[1] Juang, B. C., Laghumavarapu, R. B., Foggo, B. J., Simmonds, P. J., Lin, A., Liang, B., & Huffaker, D. L. (2015). GaSb thermophotovoltaic cells grown on GaAs by molecular beam epitaxy using interfacial misfit arrays. Applied Physics Letters, 106(11), 111101.

[2] Bett, A. W., & Sulima, O. V. (2003). GaSb photovoltaic cells for applications in TPV generators. *Semiconductor science and technology*, *18*(5), S184.

[3] Nelson, G. T., Juang, B. C., Johnston, S., Slocum, M. A., Bittner, Z. S., Lagumavarapu, R. B., ... & Hubbard, S. M. (2017, June). Investigation and Mitigation of Shunts for Higher Efficiency Epitaxial GaSb/GaSb and GaSb/GaAs Solar Cells. In *2017 IEEE 44th Photovoltaic Specialist Conference (PVSC)* (pp. 202-205). IEEE.

[4] Wei, Y., Gin, A., Razeghi, M., & Brown, G. J. (2002). Advanced InAs/GaSb superlattice photovoltaic detectors for very long wavelength infrared applications. *Applied physics letters*, *80*(18), 3262-3264.

[5] Juang, B. C., Prout, D. L., Liang, B., Chatziioannou, A. F., & Huffaker, D. L. (2016). Characterization of GaSb photodiode for gamma-ray detection. *Applied Physics Express*, *9*(8), 086401.

[6] Juang, B. C., Chen, A., Ren, D., Liang, B., Prout, D. L., Chatziioannou, A. F., & Huffaker, D. L. (2019). Energy-Sensitive GaSb/AlAsSb Separate Absorption and Multiplication Avalanche Photodiodes for X-Ray and Gamma-Ray Detection. *Advanced Optical Materials*, 1900107.

[7] Perotin, M., Coudray, P., Gouskov, L., Luquet, H., Llinares, C., Bonnet, J. J., ... & Lambert, B. (1994). Passivation of GaSb by sulfur treatment. *Journal of electronic materials*, *23*(1), 7-12.

[8] Kudrawiec, R., Nair, H. P., Latkowska, M., Misiewicz, J., Bank, S. R., & Walukiewicz, W. (2012). Contactless electroreflectance study of the Fermi level pinning on GaSb surface in n-type and p-type GaSb Van Hoof structures. *Journal of Applied Physics*, *112*(12), 123513.

[9] Carpenter, M. S., Melloch, M. R., Cowans, B. A., Dardas, Z., & Delgass, W. N. (1989). Investigations of ammonium sulfide surface treatments on GaAs. *Journal of Vacuum Science & Technology B: Microelectronics Processing and Phenomena*, *7*(4), 845-850.

[10] Bessolov, V. N., Konenkova, E. V., & Lebedev, M. V. (1997). Sulfidization of GaAs in alcoholic solutions: a method having an impact on efficiency and stability of passivation. *Materials Science and Engineering: B*, *44*(1-3), 376-379.

[11] Tajik, N., Peng, Z., Kuyanov, P., & LaPierre, R. R. (2011). Sulfur passivation and contact methods for GaAs nanowire solar cells. *Nanotechnology*, *22*(22), 225402.

[12] Ohno, T., & Shiraishi, K. (1990). First-principles study of sulfur passivation of GaAs (001) surfaces. *Physical Review B*, *42*(17), 11194.

[13] Chen, X., Xia, N., Yang, Z., Gong, F., Wei, Z., Wang, D., ... & Liao, L. (2018). Analysis of the influence and mechanism of sulfur passivation on the dark current of a single GaAs nanowire photodetector. *Nanotechnology*, *29*(9), 095201.

[14] Bessolov, V. N., Lebedev, M. V., Novikov, E. B., & Tsarenkov, B. V. (1993). Sulfide passivation of III–V semiconductors: Kinetics of the photoelectrochemical reaction. *Journal of*

Vacuum Science & Technology B: Microelectronics and Nanometer Structures Processing, Measurement, and Phenomena, *11*(1), 10-14.

[15] Kim, H. S., Plis, E., Gautam, N., Myers, S., Sharma, Y., Dawson, L. R., & Krishna, S. (2010). Reduction of surface leakage current in InAs/GaSb strained layer long wavelength superlattice detectors using SU-8 passivation. *Applied Physics Letters*, *97*(14), 143512.

[16] Wu, B., Xia, G., Li, Z., & Zhou, J. (2002). Sulphur passivation of the InGaAsSb/GaSb photodiodes. *Applied physics letters*, *80*(7), 1303-1305.

[17] Plis, E., Kutty, M. N., Myers, S., Kim, H. S., Gautam, N., Dawson, L. R., & Krishna, S. (2011). Passivation of long-wave infrared InAs/GaSb strained layer superlattice detectors. *Infrared Physics & Technology*, *54*(3), 252-257.

[18] Hood, A., Razeghi, M., Aifer, E. H., & Brown, G. J. (2005). On the performance and surface passivation of type II InAs⁄ GaSb superlattice photodiodes for the very-long-wavelength infrared. *Applied Physics Letters*, *87*(15), 151113.

[19] Huang, S., Balakrishnan, G., & Huffaker, D. L. (2009). Interfacial misfit array formation for GaSb growth on GaAs. *Journal of Applied Physics*, *105*(10), 103104.

[20] May, P. M., Batka, D., Hefter, G., Königsberger, E., & Rowland, D. (2018). Goodbye to S 2− in aqueous solution. *Chemical communications*, *54*(16), 1980-1983.

[21] Chen, S. M., & Chiu, S. W. (2000). The electrocatalytic transformation of HS−, S2O32−, S4O62− and SO32− to SO42− by water-soluble iron porphyrins. *Electrochimica acta*, *45*(27), 4399-4408.

[22] Nardelli, M. T., & Fava, G. I. O. V. A. N. I. I. A. (1962). The crystal structure of barium thiosulphate monohydrate. *Acta Crystallographica*, *15*(5), 477-484.

[23] Heslop, S. L., Peckler, L., & Muscat, A. J. (2017). Reaction of aqueous ammonium sulfide on SiGe 25%. *Journal of Vacuum Science & Technology A: Vacuum, Surfaces, and Films*, *35*(3), 03E110.

[24] Shin, J., Geib, K. M., Wilmsen, C. W., & Lilliental-Weber, Z. (1990). The chemistry of sulfur passivation of GaAs surfaces. *Journal of Vacuum Science & Technology A: Vacuum, Surfaces, and Films*, *8*(3), 1894-1898.

[25] Lunt, S. R., Santangelo, P. G., & Lewis, N. S. (1991). Passivation of GaAs surface recombination with organic thiols. *Journal of Vacuum Science & Technology B: Microelectronics and Nanometer Structures Processing, Measurement, and Phenomena*, *9*(4), 2333-2336.

[26] Bessolov, V. N., Konenkova, E. V., & Lebedev, M. V. (1996). Solvent effect on the properties of sulfur passivated GaAs. *Journal of Vacuum Science & Technology B: Microelectronics and Nanometer Structures Processing, Measurement, and Phenomena*, *14*(4), 2761-2766.

[27] Alexander-Webber, J. A., Groschner, C. K., Sagade, A. A., Tainter, G., Gonzalez-Zalba, M. F., Di Pietro, R., ... & Joyce, H. J. (2017). Engineering the photoresponse of InAs nanowires. *ACS applied materials & interfaces*, *9*(50), 43993-44000.

[28] Higuera-Rodriguez, A., Romeira, B., Birindelli, S., Black, L. E., Smalbrugge, E., Van Veldhoven, P. J., ... & Fiore, A. (2017). Ultralow surface recombination velocity in passivated InGaAs/InP nanopillars. *Nano letters*, *17*(4), 2627-2633.

[29] Salihoglu, O., Muti, A., Kutluer, K., Tansel, T., Turan, R., Kocabas, C., & Aydinli, A. (2012). Atomic layer deposited Al2O3 passivation of type II InAs/GaSb superlattice photodetectors. *Journal of Applied Physics*, *111*(7), 074509.

[30] Chen, A., Juang, B. C., Ren, D., Liang, B., Prout, D. L., Chatziioannou, A. F., & Huffaker, D. L. (2019). Significant suppression of surface leakage in GaSb/AlAsSb heterostructure with Al2O3 passivation. *Japanese Journal of Applied Physics*, *58*(9), 090907.